Pyriproxyfen and diflubenzuron pesticides impair human adipose stem cell function: evidence of redox imbalance, KDM6B upregulation, and dysregulated adipogenesis

Food and Chemical Toxicology 212 (2026) 116057

Contents lists available at ScienceDirect

Food and Chemical Toxicology

journal homepage: www.elsevier.com/locate/foodchemtox

Pyriproxyfen and diflubenzuron pesticides impair human adipose stem cell function: evidence of redox imbalance, KDM6B upregulation, and dysregulated adipogenesis

Ana Beatriz Marques Abel [a], Andressa França Sousa Bispo [b], Jussara de Jesus Simao [b], Artur Francisco da Silva Neto [a], Julia Fernandes Barcella [c], Lila Missae Oyama [a], Bruno Fiorelini Pereira [d], Allain Amador Bueno [e,*], Maria Isabel Cardoso Alonso-Vale [a,b,d]

[a] Post-Graduate Program in Nutrition - Paulista School of Medicine, Federal University of São Paulo - UNIFESP, Sao Paulo, 04023-062, Brazil
[b] Post-Graduate Program in Chemical Biology - Institute of Environmental Sciences, Chemical and Pharmaceutical - ICAQF, UNIFESP, Diadema, 09913-030, Brazil
[c] Undergraduate Program in Pharmacy and Biochemistry, ICAQF, UNIFESP, Diadema, 09913030, Brazil
[d] Department of Biological Sciences, Institute of Environmental Sciences, Chemical and Pharmaceutical, Federal University of São Paulo - UNIFESP, Diadema, 09913-030, Brazil
[e] College of Health, Life and Environmental Sciences, University of Worcester, Worcester, WR2 6AJ, United Kingdom

ARTICLE INFO

Handling Editor: Professor Matthew Wright

Keywords:
Metabolic dysfunction
Chemokines
Epigenetic regulation
MCP1
Endocrine disruption

ABSTRACT

Introduction: Pyriproxyfen (PPF) and diflubenzuron (DFB) are widely used pesticides with metabolic toxicity in humans underexplored. White adipose tissue (WAT) is a potential target for endocrine-disrupting chemicals.
Aim: We investigated the effects of PPF and DFB on human adipose-derived stem cells (hASCs) redox balance, epigenetic regulation, and adipogenic differentiation.
Method: Visceral WAT hASCs were exposed to PPF or DFB (0.01–2 mg/L). Cytotoxicity was observed at ≥1.5 mg/L, with 1 mg/L selected for further experiments.
Results: 8-day exposure to PPF or DFB reduced catalase and superoxide dismutase activities while increasing glutathione peroxidase. This was accompanied by 74% increase in mRNA expression of H3K27 demethylase KDM6B and elevated secretion of CCL2 in PPF-exposed cells. During adipogenic differentiation, PPF and DFB upregulated early transcription factors and enhanced lipid accumulation. Differentiated adipocytes exhibited higher proportion of saturated fatty acids and increased leptin secretion, while adiponectin levels remained unchanged. In mature primary adipocytes, PPF suppressed the secretion of leptin and adiponectin, and significantly increased basal lipolysis.
Discussion: our results show endocrine and metabolic disruption induced by non-cytotoxic concentrations of PPF and DFB. PPF upregulated the epigenetic modulator KDM6B and promoted dysregulated adipogenic programming in hASCs, favouring lipid accumulation and a pro-inflammatory, metabolically compromised phenotype.

1. Introduction

Pyriproxyfen (PPF) and diflubenzuron (DFB) are pesticides widely used worldwide, commonly employed in agriculture and for managing pests such as whiteflies (Porretta et al., 2019; Qin and Hu, 2023; Cabral et al., 2024) and the *Aedes aegypti* mosquito. PPF acts as a juvenile hormone analogue, disrupting insect development (Ur Rahman et al., 2024), while DFB inhibits chitin synthesis, thereby impeding the growth of larvae and pests such as mosquitoes, cotton caterpillars, and flies (de Abreu et al., 2025). The World Health Organization (WHO) has formally endorsed the use of both compounds for pest control (World Health Organization, 2022a, 2022b).

However, their environmental persistence and biological activity raise concerns about potential effects on non-target organisms. For instance, exposure of zebrafish embryos to DFB (0–4.5 mg/L) leads to increased mortality, cardiac malformations, oxidative stress, and

* Corresponding author. College of Health, Life and Environmental Science, University of Worcester, Henwick Grove, Worcester, United Kingdom.
E-mail addresses: anabeatrizmarquesabel@gmail.com (A.B.M. Abel), andressa.franca@unifesp.br (A.F.S. Bispo), jussara.simao@unifesp.br (J.J. Simao), artur.francisco@unifesp.br (A.F. Silva Neto), julia.barcella@unifesp.br (J.F. Barcella), lmoyama@gmail.com (L.M. Oyama), bf.pereira@unifesp.br (B.F. Pereira), a.bueno@worc.ac.uk (A.A. Bueno), alonso.vale@unifesp.br (M.I.C. Alonso-Vale).

https://doi.org/10.1016/j.fct.2026.116057
Received 23 January 2026; Received in revised form 6 March 2026; Accepted 7 March 2026
Available online 10 March 2026

apoptosis (Han et al., 2022). More critically, a study in *Lithobates catesbeianus* frogs showed that PPF exposure (2–20 mg/L) accumulates in white adipose tissue (WAT) even at concentrations near the WHO-recommended dose (Nimet et al., 2021), a range frequently cited as 0.01 to 0.05 mg/L for water treatment in breeding sites. These findings highlight WAT as a significant reservoir for lipophilic environmental toxins, including pesticides.

WAT is known to accumulate toxic substances from soil, water, and air, which can negatively affect adipocyte function (Jackson et al., 2017). Studies on persistent pollutants such as organophosphate pesticides (OPPs) and organophosphate esters (OPEs) have demonstrated their accumulation in both subcutaneous and visceral WAT of obese women, where they correlate with altered adipose tissue hormonal secretion (Jackson et al., 2017). These effects may extend beyond mature adipocytes to the adipose-derived stem cells (ASCs) residing in the vascular stromal fraction. ASCs are essential for WAT plasticity, facilitating differentiation into mature adipocytes and adipogenesis (Lecoutre et al., 2025; Suchanecka et al., 2025a,b).

Dysfunctional adipogenesis is a key event in the development of metabolically unhealthy obesity, characterized by altered adipokine secretion such as reduced adiponectin and elevated leptin, chronic inflammation, and insulin resistance (Engin, 2024; Matar et al., 2025). Critically, exposure to environmental pollutants can disrupt ASC biology, skewing adipogenesis toward a pro-inflammatory and metabolically compromised phenotype.

Despite evidence of bioaccumulation, the specific effects of PPF and DFB on human adipose-derived stem cells (hASC) metabolism remain largely unknown, with their potential to induce oxidative stress and subsequently trigger epigenetic reprogramming yet to be elucidated. This gap in knowledge is significant, as oxidative stress can modulate the activity of epigenetic regulators such as the histone 3 lysine (H3K27) Lysine Demethylase 6 B (KDM6B), thereby influencing gene expression programs critical for adipocyte differentiation and function (Simão et al., 20240; Bispo et al., 2025; Bu et al., 2025).

Therefore, this study aimed to test the hypothesis that chronic exposure to PPF or DFB impairs hASC metabolism by disrupting redox balance and epigenetic regulation, leading to dysregulated adipogenesis. We investigated their effects on: (1) cell viability and components of the antioxidant defence system (antioxidant enzyme activities); (2) the expression of the epigenetic modulator Jumonji D3 (JMJD3), also known as KDM6B, and associated inflammatory signals; and (3) adipogenic differentiation, lipid metabolism, and adipokine secretion. Our findings provide novel mechanistic insights into how these common pesticides may contribute to adipose tissue dysfunction and metabolic risk.

2. Materials and methods

All chemicals were purchased from Sigma-Aldrich (St. Louis, MO, USA), including general reagents (e.g., buffers and solvents) and specialized chemicals such as PPF and DFB, as well as those used for chromatography, spectroscopy, and molecular biology, unless otherwise stated.

2.1. Collection of patient samples

The study protocol was approved by the Research Ethics Committee of the Federal University of São Paulo (CEP/UNIFESP Project No. 0268/2022; approval date: June 7, 2022; CAAE: 57087422.8.0000.5505), and authorization for sample collection at Hospital São Luiz was granted under Ethics Opinion No. 7.640.160.

Visceral white adipose tissue (vWAT) samples were obtained from the omentum region. These samples were collected from four male patients, aged 30-50 years, with a body mass index (BMI) between 25 and 27 kg/m^2, who underwent elective surgery at Hospital São Luís do Itaim (São Paulo, Brazil). All participants provided written informed consent prior to enrolment by signing the Free and Informed Consent Form. Participant eligibility was determined according to pre-established inclusion criteria based on WHO guidelines (World Health Organization, 2023). Collected samples were transported in sterile phosphate buffered saline (PBS), maintained at 4 °C in an insulated container, and processed within 2 h of collection.

2.2. Processing of adipose tissue for human adipocytes and hASC isolation

Following dissection and fragmentation of vWAT, according to an established method with specific modifications for this study (Bellei et al., 2017), the tissue was placed in digestion buffer [Dulbecco's modified Eagle's medium - D'MEM/HEPES 20 mM/bovine serum albumin (BSA) 4%, collagenase II - 1.0 mg/ml, pH 7.40]. Incubation took place for around 10-15 min at 37 °C in a water bath with orbital shaking (130 rpm) to digest the tissue. Samples were transferred to 50 mL falcon tubes and the volume completed to 25 mL with [25 mM EARLE/HEPES (EHB) salts, 1% BSA, 1 mM sodium pyruvate, without glucose, pH 7.45, 37 °C]. The filtrate was centrifuged (400 g, 1 min) and divided into two fractions: the upper layer or supernatant, which contains the isolated primary adipocytes, and the stromal vascular fraction (SVF), which contains the hASCs precursor cells.

The first fraction was used for morphometric analysis, where aliquots of this adipocyte suspension were examined under an optical microscope with a graduated eyepiece to measure the average diameter of 100 cells. Assuming a spherical shape, the average cell volume (in pL) was calculated using formula $V = (\pi/6) \times D^3/10^3$, where D is the average diameter in μm (Rodbell, 1964).

The SVF, which contains the hASCs precursor cells, were pelleted from the initial centrifugation and subjected to further centrifugation (1500 g for 5 min). The new pellet was washed with EHB buffer and centrifuged twice more. Finally, it was resuspended in complete culture medium [DMEM Han's F-12 supplemented with 10% foetal bovine serum (FBS) and 1% penicillin/streptomycin (P/S)] and plate. Cultures were maintained at 37 °C in a 5% CO_2 atmosphere. The medium was refreshed every two days. After this period, the medium was removed, and the cells were washed PBS. The final step for isolation of hASCs is the selection of the adherent SVF population. This population of hASCs obtained for the first time is considered passage "0" (P0). Following removal of the medium and a PBS rinse, the adherent SVF population, which represents the hASCs, was detached using trypsin. These cells at passage 1 (P1) were resuspended and transferred to larger culture vessels for further expansion, maintaining the same confluence threshold. Cell counts were performed using a Neubauer chamber to monitor density. Subsequent confirmation of hASC identity was achieved via immunophenotyping, which demonstrated a population positive for 5′-nucleotidase ecto (CD73) and Cluster of Differentiation 90 (CD90) and negative for Platelet Endothelial Cell Adhesion Molecule-1 (CD31) and Leukocyte Common Antigen (CD45) (>95% purity; data not shown).

2.3. Exposure of cells to PPF/DFB and MTT assay

One mg of PPF or DFB (PESTANAL®, analytical standard, CAS 95737-68-1 and CAS 35367-38-5, respectively) was dissolved in one mL of dimethyl sulfoxide (DMSO) to prepare the stock solution. Serial dilutions in culture medium were then performed to obtain the final working concentrations of 0.05, 0.1, 1, 1.5, and 2 mg/L. For hASCs, cells were seeded in 96-well plates at a density of 5×10^3 cells/well in 100 μL of complete medium (D'MEM Han's F-12/10% FBS/1% P/S). After reaching 100% confluence, cells were exposed to the respective concentrations of PPF or DFB for 48 h, 96 h, 6 days, and 8 days. The potential effect of PPF (0.05 to 2 mg/L) on ASC differentiation was also evaluated over an 8-day period. Primary adipocytes isolated as described in section 2.2 were similarly exposed to the compound concentrations for a 96-h period. Cells treated with 0 means absence from

PPF or DFB. Cell viability was assessed using the 3-[4,5-dimethylthiazol-2-yl]-2,5-diphenyltetrazolium bromide (MTT) reduction assay, reduction assay (Denizot and Lang, 1986). Following each exposure period, a 10 μL volume of MTT solution (5 mg/mL in PBS) was added to each well. The plates were then incubated for 4 h at 37 °C in a 5% CO_2 atmosphere to allow formazan crystal formation. Subsequently, 100 μL of the solubilization solution 10% sodium dodecyl sulphate in 0.01 M Hydrochloric acid (HCl)] was added to each well. Plates were incubated for an additional 16 h under the same conditions to fully dissolve the crystals. Absorbance was measured at 550 nm using a microplate reader. Results were expressed as a percentage of viability relative to the untreated control group.

2.4. Adipogenic differentiation

For differentiation, hASCs were cultured until they reached 100% confluence. Upon reaching confluence (designated as day 0, D0), adipogenic differentiation was induced by treatment with an induction medium. This medium consisted of DMEM/Ham's F-12 supplemented with an adipogenic cocktail containing 0.5 mM 3-isobutyl-1-methylxanthine (IBMX), 0.1 μM dexamethasone, 0.5 μM human insulin, 2 nM triiodothyronine (T3), 30 μM indomethacin, 17 μM pantothenate, 33 μM biotin, 1 μM rosiglitazone, 1 mg/mL apo-transferrin, 2% FBS, and 1% P/S. The cells were maintained in this medium for either 8 or 20 days, in the absence or presence of PPF or DFB, at concentrations selected based on the MTT assay results.

2.5. Staining with red oil O and determination of lipid content

hASCs were differentiated in 6-well plates for 20 days in the absence or presence of PPF 1 mg/L. Following this period, the cells were washed twice with PBS and fixed with 10% formalin in PBS for 15 min. After another PBS wash, the samples were stained for 1 h with a freshly prepared 0.3% Oil Red O solution in 60% (v/v) isopropanol. This staining was performed to label, visualize, and quantify the intracellular lipid content, intracellular lipid content (Fei et al., 2011). The staining solution was then removed, and the cells were washed twice with 2 mL of distilled water. Finally, the cells were destained with 60% isopropanol and photographed. Imaging was performed using an inverted microscope equipped with AxioVision software (AxioVision 4, Zeiss, Goettingen, Germany). For quantification, the incorporated dye was eluted with 100% ethanol, and its optical density was measured spectrophotometrically at 540 nm.

2.6. Enzyme-linked immunosorbent assay (ELISA)

The concentrations of monocyte chemoattractant protein-1 (CCL2/MCP1), leptin, and adiponectin in the culture medium following PPF or DFB exposure were quantified using commercially available ELISA kits (Quantikine M; R&D Systems, Minneapolis, MN, USA).

2.7. Lipid profile analysis

ASCs were cultured until confluence and induced to adipogenic differentiation for 10 days in the presence or absence of PPF (1 mg/L). Total lipids were extracted using a sequential solvent extraction protocol adapted from (Schreiner et al., 2006). Briefly, cells were homogenized in chloroform: methanol (1:1, v/v), followed by extraction with chloroform: methanol:water (1:2:1, v/v/v). The combined extracts were evaporated to dryness under a gentle nitrogen stream. Lipids were transmethylated to fatty acid methyl esters (FAMEs), which were analysed by gas chromatography with flame ionization detection (GC-FID) using analytical-grade reagents.

2.8. Enzyme activity assay

Following an eight-day exposure to 1 mg/L PPF or DFB, cells were harvested by scraping in 150 μL of ice-cold potassium phosphate buffer [19% Monopotassium phosphate (KH_2PO_4) and 81% Dipotassium phosphate (K_2HPO_4), pH 7.4]. The resulting cell lysates were then used for the determination of antioxidant enzyme activities. Catalase (CAT) activity was measured spectrophotometrically by monitoring the decomposition rate of hydrogen peroxide (H_2O_2) at 240 nm. The enzymatic activity was quantified by comparison with a standard curve prepared from known concentrations of H_2O_2. Enzyme activities were assessed using commercially available kits: superoxide dismutase (SOD) activity was measured using the RANSOD kit (Randox®, Cat. No. SD 125/MD, Randox Laboratories Ltd., Crumlin, UK), and glutathione peroxidase (GPx) activity was measured using the RANSEL kit (Randox®, Cat. No. RS 504/MD, Randox Laboratories Ltd., Crumlin, UK), following the manufacturer's instructions to account for differences in cell number across samples, all enzyme activities (CAT, SOD, and GPx) were normalized to the total protein content of each corresponding lysate. Total protein concentration was determined using the bicinchoninic acid (BCA) assay. Results are expressed as units per milligram of protein (U/mg protein).

2.9. Lipolysis assay

Basal lipolytic activity was assessed in primary adipocytes by quantifying glycerol release into the incubation medium. Adipocytes were first treated with 1 mg/L PPF or vehicle for 96 h. After exposure, cells were washed and incubated for 30 min at 37 °C in Krebs Ringer-phosphate buffer (pH 7.4) containing 20 mM BSA and 5 mM glucose to stimulate basal lipolysis. The reaction was stopped on ice, and medium aliquots were collected. Glycerol concentration was determined using enzymatic assay (Free Glycerol Determination Kit), with absorbance measured at 540 nm. Cell number for normalization was estimated based on the average cell volume (pL), which was derived from the morphometric analysis of adipocyte diameter described in Section 2.2. Results are expressed as nanomoles (nmol) of glycerol released per 10^6 cells.

2.10. RNA extraction and quantitative real-time PCR

hASCs were cultured for eight days in the presence of PPF or DFB at a concentration of 1 mg/L. Total RNA was then extracted using TRIzol reagent (Invitrogen Life Technologies, Carlsbad, CA, USA) according to the manufacturer's instructions. The RNA concentration and purity were assessed spectrophotometrically at 260 nm using a NanoDrop instrument (Thermo Scientific, Walthamm, MA, USA). RNA samples were stored at −80 °C until further processing. For cDNA synthesis, 1 μg of total RNA was reverse transcribed using oligo (dT) primers and the SuperScript III Reverse Transcriptase kit (Thermo Scientific, Walthamm, MA, USA) in the presence of dNTPs, following the manufacturer's protocol. Quantitative real-time PCR (qPCR) was performed on a Rotor-Gene thermocycler (Qiagen) using the SYBR Green PCR kit (Qiagen). The reaction conditions were as follows: initial denaturation at 95 °C for 5 min, followed by 40 cycles of denaturation at 95 °C for 5 s and annealing/extension at 60 °C for 10 s. Gene expression levels were normalized to the housekeeping gene Glyceraldehyde-3-phosphate dehydrogenase (*GAPDH)* and calculated using the 2–ΔΔCt method. The primers used were as

Follows: *GAPDH*: forward 5′-GTCTCCTCTGACTTCAACAGC-3′, reverse 5′ACCACCCTGTTGCTGTAGCCAA-3′; *KDM6B*: forward 5′-CTCAACTTGGGCCTCTTCTC-

3′, reverse 5′-GCCTGTCAGATCCCAGTTCT-3′; CCAAT/enhancer binding protein alpha (*CEBPA)*: forward 5′CAAGAACAGCAACG AGTACCG-3′, reverse 5′-GTCACTGGTCAGCTCCAGCAC-3; CCAAT/enhancer-binding protein beta (*CEBPB)*: forward 5′-

CTTCAGCCCGTACCTGGAG-3′, reverse 5′-

GGAGAGGAAGTCGTGGTGC-3′; Krüppel-like factor 15 (*KLF15)*: forward 5′-GGTGAAAAGCGTCCCCCACT-3′, reverse 5′-TGTCTGGGAAA CCGGAGGAG-3′3.

2.11. Statistical analysis

Data are presented as the mean ± standard error of the mean (SEM). Statistical comparisons were performed using GraphPad Prism version 9.1 (GraphPad Software, Inc., San Diego, CA, USA). For comparisons between two groups, an unpaired Student's *t-test* was applied. For comparisons among three or more groups, a one-way analysis of variance (ANOVA) was conducted, followed by Tukey's post hoc test when the ANOVA indicated a significant difference. A p-value of less than 0.05 was considered statistically significant.

3. Results

3.1. Toxicity and cell viability of PPF and DFB in hASCs

Cell viability was assessed by MTT assay following exposure to PPF or DFB (0.05–2 mg/L) for 48 h, 96 h, 6 days, and 8 days. Both compounds induced a concentration dependent decrease in hASC viability. A significant reduction in viability was consistently observed at concentrations of 1.5 and 2 mg/L for all exposure periods (Fig. 1A–H). In contrast, the concentration of 1 mg/L did not cause significant cytotoxicity at any time point compared to the control. Therefore, this non-cytotoxic concentration (1 mg/L) was selected for all subsequent experiments to investigate the specific effects of PPF and DFB on hASC function without the confounding factor of overt cell death. This concentration was chosen also because it reflects levels already tested in other cell lines and *in vivo* models including zebrafish, mice, and rats (Lee et al., 2021; Cabral et al., 2024).

3.2. PPF and DFB exposure impairs antioxidant defences and upregulates the epigenetic modulator KDM6B in hASCs

Exposure of hASCs to PPF and DFB significantly reduced the activity of key antioxidant enzymes: SOD decreased by 8.84% and 46.9 % (Fig. 2A and D), and CAT by 3.7% and 8.2 % (Fig. 2B and E), respectively, whereas GPx activity increased by 18.4% and 22.9% (Fig. 2C and F). This selective impairment indicates a disruption of cellular redox homeostasis.

Given the established role of reactive oxygen species (ROS) as mediators of epigenetic reprogramming (He et al., 2016; Kietzmann et al., 2017; Bu et al., 2025), we investigated the expression of KDM6B, an H3K27 demethylase known to be sensitive to redox changes. Quantitative analysis revealed a marked, 74% increase in KDM6B transcript levels in hASCs exposed to PPF (Fig. 2G). In line with previous findings linking KDM6B activity to inflammatory pathways, this upregulation was associated with increased secretion (14.3 %) of the proinflammatory chemokine CCL2/MCP-1 (Fig. 2H).

3.3. Exposure to PPF and DFB during proliferation upregulated the expression of early transcription factors in hASCs prior to differentiation

To determine whether the pesticides could alter adipogenic programming prior to adipogenic induction, we analysed the expression of key adipogenic regulators following eight days of exposure during proliferation and confluence, but before adipogenic induction. Pre-exposure to PPF (1 mg/L) significantly increased the mRNA levels of the early transcription factors *KLF15* and *CEBPB*. Similarly, DFB exposure upregulated the expression of *KLF15* and *CEBPA* (Fig. 3).

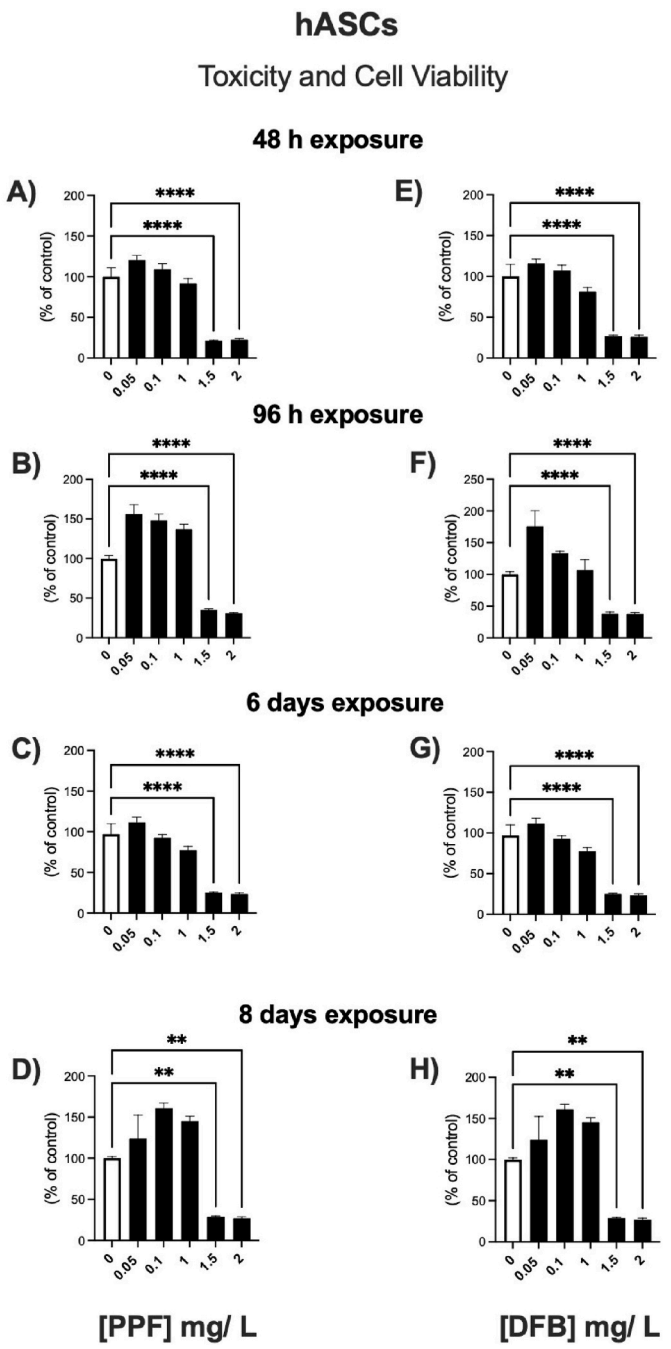

Fig. 1. Cytotoxicity of PPF and DFB in hASCs. Cell viability was assessed by MTT assay after exposure to increasing concentrations (0.05–2 mg/L) of (**A-D**) PPF or (**E-H**) DFB for 48 h, 96 h, 6 days, and 8 days. Data are expressed as a percentage of the control (untreated) group. Mean ± SEM from n = 2 independent human donors (biological replicates), each assayed in technical triplicate. $^{**}p < 0.001$, $^{****}p < 0.00001$ (One-way ANOVA followed by Tukey's post-test).

3.4. PPF and DFB enhance lipid accumulation and alter adipocyte phenotype during differentiation

Given the evidence of early adipogenic programming, we induced adipogenic differentiation in the continuous presence of PPF. This chronic exposure resulted in a significant increase in lipid accumulation in mature adipocytes, as quantified by Oil Red O staining (Fig. 4A). Analysis of the lipid composition by gas chromatography revealed a consistent trend (despite the limited sample size, n = 4) toward a higher

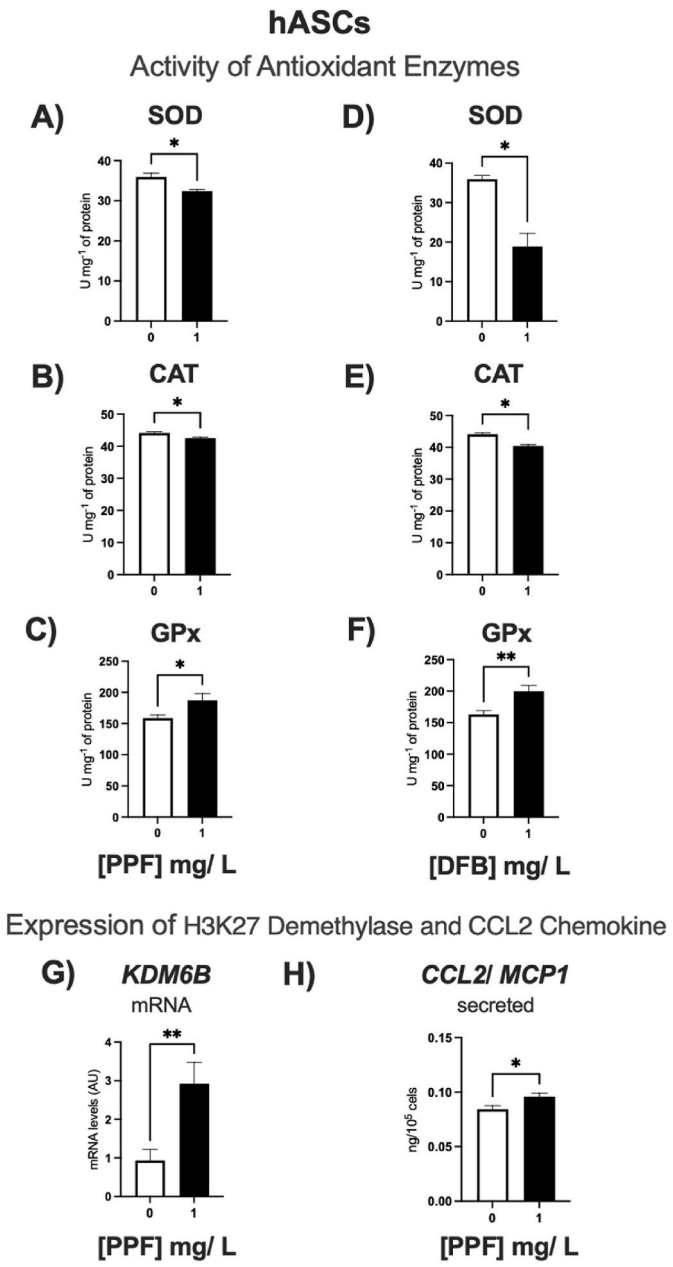

Fig. 2. Antioxidant enzyme activity, *KDM6B* expression, and CCL2 secretion in hASCs exposed to PPF or DFB. (**A–C**) Activity of catalase (CAT), superoxide dismutase (SOD), and glutathione peroxidase (GPx) in hASCs treated with PPF (1 mg/L) for 8 days. (**D–F**) Activity of CAT, SOD, and GPx in hASCs treated with DFB (1 mg/L) for 8 days. (**G**) *KDM6B* mRNA levels, expressed in arbitrary units (AU) and normalized to GAPDH. (**H**) Secreted CCL2 protein levels. Mean ± SEM from n = 4 independent human donors (biological replicates), each assayed in technical triplicate. *$p < 0.05$, **$p < 0.001$ (Student's *t*-test).

proportion of myristic and palmitic acid, and consequently of total saturated fatty acids, in PPF-treated cells (Fig. 4B).

At the molecular level, this enhanced lipid-storage phenotype was accompanied by increased expression of the late adipogenic marker leptin after 8 days of differentiation (Fig. 4C). In contrast, the expression of adiponectin—a key adipokine associated with metabolic health—remained unchanged (Fig. 4D). This specific pattern of marker expression (elevated leptin, unchanged adiponectin) indicates a dysregulated adipogenic process. Importantly, the same phenotype—increased lipid accumulation with elevated leptin but unchanged adiponectin—was fully replicated in adipocytes differentiated under continuous DFB exposure (Fig. 4E–F).

3.5. PPF does not affect viability but increases lipolysis and decreases adipokine secretion by human primary adipocytes

To assess the direct impact of PPF on mature adipocyte function, we first evaluated cell viability after a 96-h exposure to a concentration range (0.05–2 mg/L). The MTT assay revealed no cytotoxic effects at any concentration tested compared to the untreated control (Fig. 5A). Based on this non-cytotoxic profile, we selected the concentration of 1 mg/L to investigate the compound's effect on adipocyte metabolism and endocrine function.

Exposure to 1 mg/L PPF significantly increased basal lipolysis by 38%. Interestingly, in contrast to its effect on newly differentiated adipocytes derived from hASCs, PPF reduced the secretion of key adipokines in mature primary adipocytes, decreasing leptin by 25% (Fig. 5B) and adiponectin by 25% (Fig. 5C). This distinct, cell-context-dependent response suggests that PPF simultaneously promotes lipid mobilization and impairs the endocrine function of mature fat cells, while inducing a dysregulated secretory phenotype during the differentiation of progenitor cells.

4. Discussion

Our study describes a multi-faceted adverse outcome pathway in hASCs exposed to the pesticides PPF and DFB. The exposure triggered a cascade of unfavourable events, initiated by redox imbalance, progressing through epigenetic and proinflammatory reprogramming, and culminating in dysregulated adipogenic commitment and a dysfunctional adipocyte phenotype.

First, we observed that chronic exposure significantly reduced the activity of key antioxidant enzymes, specifically SOD and CAT. This attenuation suggests a possible scenario of ROS accumulation and consequent disturbance in cellular redox homeostasis (Zorov et al., 2014). ROS are established mediators of epigenetic reprogramming (He et al., 2016; Kietzmann et al., 2017) and can induce the expression of the histone demethylase KDM6B via ROS-sensitive pathways, such as STAT6 (He et al., 2016). KDM6B removes repressive marks (H3K27me3) and recruits acetylases to add activating marks (H3K27ac), promoting the expression of genes, including antioxidants and proinflammatory genes (Chen et al., 2017; He et al., 2016; Kietzmann et al., 2017; Sun et al., 2021; Bu et al., 2025).

Supporting this mechanistic link, our analysis revealed a substantial upregulation of KDM6B transcript levels in PPF-exposed hASCs. This aligns with a recent mechanistic study, which established that H3K27 demethylation, catalyzed by the KDM6B enzyme, is a critical event for CCL2 upregulation in LPS-stimulated mononuclear cells (Akhter et al., 2022). It also aligns with prior work from our group, which links elevated KDM6B to increased H3K27 acetylation and the upregulation of proinflammatory genes (Simão et al., 2024). Guided by this established pathway, we hypothesized that pesticide exposure might similarly engage this mechanism in hASCs, thereby extending the relevance of the KDM6B-CCL2 axis to an environmental toxicant model in human mesenchymal cells. It is important to note, however, that this study did not delve into the functional validation of this mechanism. While the correlation with existing literature is compelling, further mechanistic studies are essential to establish a causal link. Specifically, experiments involving KDM6B inhibition are required to determine if this epigenetic modifier is directly responsible for the CCL2 upregulation observed upon PPF exposure.

Interestingly, the proinflammatory shift was accompanied by a concurrent, yet seemingly insufficient, antioxidant response, as evidenced by an increase in GPx activity alongside declines in SOD and CAT. This pattern points to a state of redox imbalance, suggesting that the antioxidant system is overwhelmed, which may in turn exacerbate the pro-inflammatory state — a response conserved across models, as

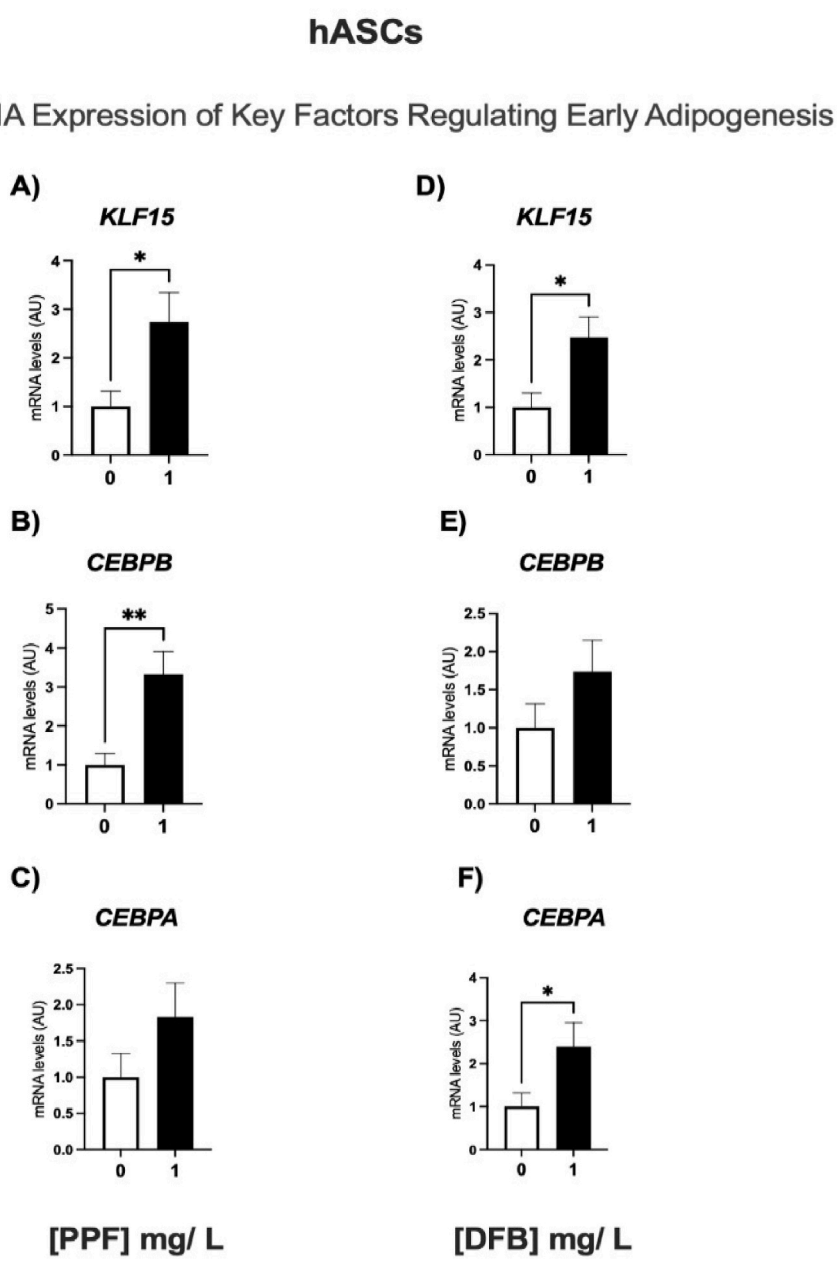

Fig. 3. mRNA expression of early adipogenic transcription factors in hASCs exposed to PPF or DFB. (**A–C**) Expression of *KLF15*, *CEBPB*, and *CEBPA* by hASCs treated with PPF (1 mg/L) for 8 days. (**D–F**) Expression of *KLF15*, *CEBPB*, and *CEBPA* by hASCs treated with DFB (1 mg/L) for 8 days. Mean ± SEM from n = 4 independent human donors (biological replicates), each assayed in technical triplicate. Data were expressed in arbitrary units (AU) and normalized to GAPDH. $*p < 0.05$, $**p < 0.001$ (Student's *t*-test).

zebrafish exposed to PPF/DFB similarly exhibit adaptive upregulation of antioxidant enzymes (Teixeira et al., 2024).

Beyond inflammation and oxidative stress, PPF and DFB directly influenced cellular fate by upregulating key early transcriptional drivers of adipogenesis. PPF increased *KLF15* and *CEBPB*, while DFB induced *KLF15* and *CEBPA*. The consistent induction of *KLF15*, a critical gatekeeper of differentiation (Lin et al., 2023), suggests that both pesticides promote adipogenic commitment. This transcriptional reprogramming manifested phenotypically as enhanced lipid accumulation, confirmed by Oil Red O staining, and increased secretion of the adipokine leptin—a hallmark of mature adipocytes (Obradovic, 2021). In addition, fatty acid profiling revealed higher levels of myristic acid in adipocyte cell with PPF compared to absence PPF, reinforcing the alterations in lipid metabolism associated with adipocyte maturation. Significantly, however, this adipogenic program was metabolically impaired. We observed a dissociation in adipokine secretion: leptin levels increased, while adiponectin—an insulin-sensitizing, anti-inflammatory hormone central to metabolic health—remained unchanged. This specific pattern of elevated leptin without a proportional increase in adiponectin is a recognized signature of dysfunctional, hypertrophic WAT (Gao et al., 2025). Notably, this precise endocrine disruption was reported in adult bullfrogs (*Lithobates catesbeianus*) with PPF bioaccumulation in WAT (Nimet et al., 2021). The concordance of this adipokine imbalance across vertebrate classes strengthens its biological and toxicological relevance.

Intriguingly, the endocrine effect of PPF was strictly dependent on the cellular differentiation state. While it increased leptin secretion during the adipogenic differentiation of hASCs, exposure to mature primary human adipocytes elicited an opposite response, suppressing the secretion of both leptin and adiponectin. This result indicates that

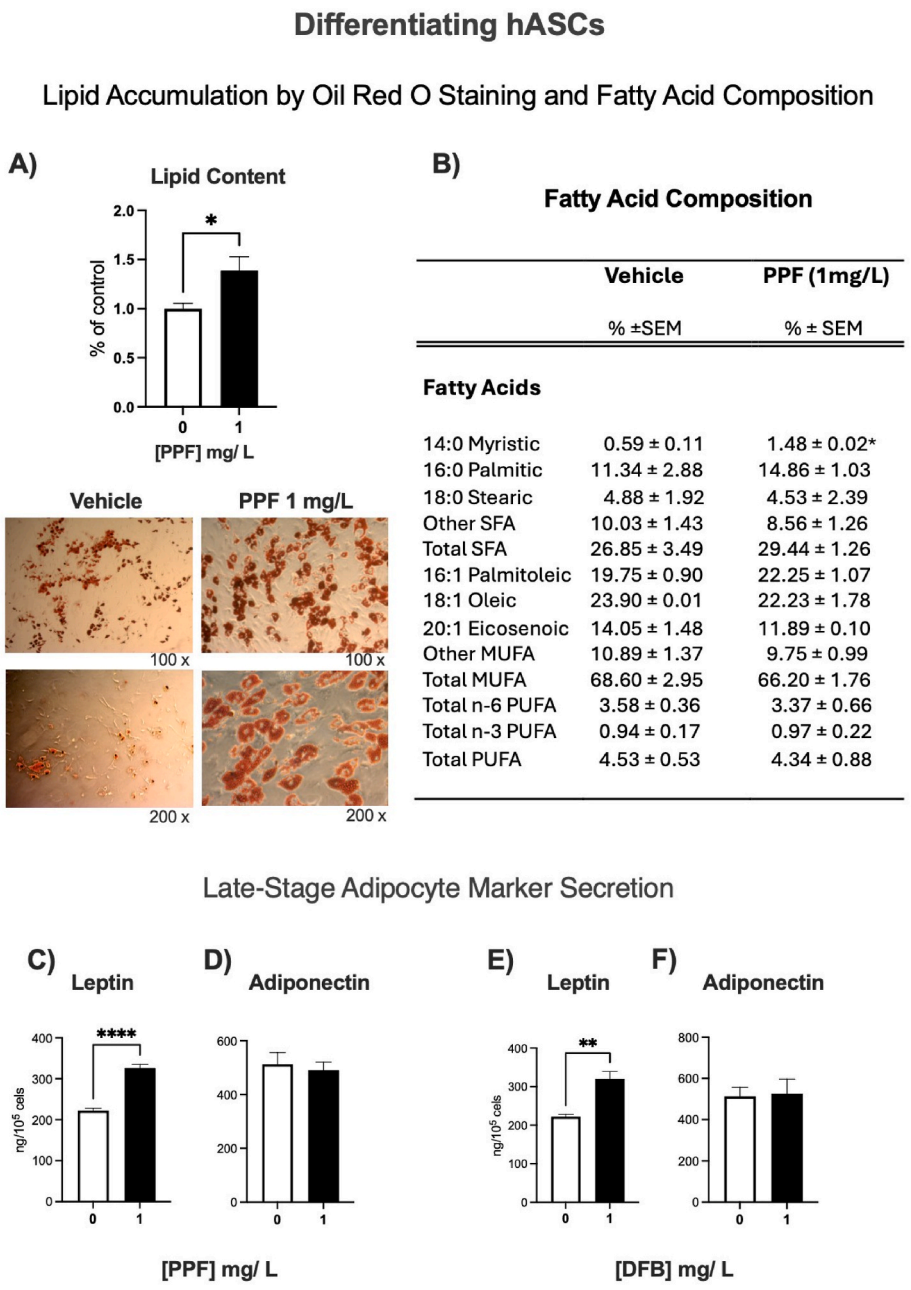

Fig. 4. Lipid accumulation, fatty acid composition, and adipokine secretion in hASCs differentiated with PPF or DFB. (**A**) Lipid accumulation (Oil Red O) in hASCs differentiated with or without PPF (1 mg/L) for 20 days. Data are expressed as a percentage of the control (untreated) group. Representative images of stained cells are shown below the graph. (**B**) Fatty acid composition, expressed as percentage of total fatty acids, determined as FAMEs by gas GC-FID in hASCs differentiated with PPF (1 mg/L) for 10 days. SFA: saturated fatty acids; MUFA: monounsaturated fatty acids; PUFA: polyunsaturated fatty acids. (**C–D**) Secreted leptin and adiponectin by hASCs differentiated with PPF (1 mg/L). (**E–F**) Secreted leptin and adiponectin by hASCs differentiated with DFB (1 mg/L). Mean ± SEM from n = 4 independent human donors (biological replicates), each assayed in technical triplicate. *$p < 0.05$, **$p < 0.001$, ****$p < 0.00001$ (Student's *t*-test). (For interpretation of the references to colour in this figure legend, the reader is referred to the Web version of this article.)

PPF not only dysregulates but also actively inhibits the endocrine function of mature fat cells. This cell context-dependent duality—promoting a dysfunctional secretory profile in developing adipocytes while suppressing hormone output in mature ones—reveals a more complex endocrine-disrupting mechanism that could impair adipose tissue communication at multiple physiological levels. Consistently, in mature adipocytes exposed to PPF, the lipolysis assay demonstrated a significant increase in basal glycerol release compared to non-exposed adipocytes, indicating enhanced basal lipolytic activity. Metabolically, this finding suggests a disruption of lipid homeostasis, a condition closely associated with adipose tissue dysfunction and systemic metabolic imbalance (Morigny et al., 2016).

While no prior studies have specifically investigated the effects of PPF or DFB on human adipose cells, research in other models provides crucial context and mechanistic support for our findings. Notably, a conserved theme across these studies is the induction of oxidative stress as a primary insult, aligning with our observation of redox imbalance in hASCs.

For PPF, evidence points to multifaceted toxicity. In vitro genotoxicity assays in human lymphocytes show that PPF directly induces chromosomal damage and micronuclei formation, unlocked, whereas its mutagenic potential is revealed only upon metabolic activation,

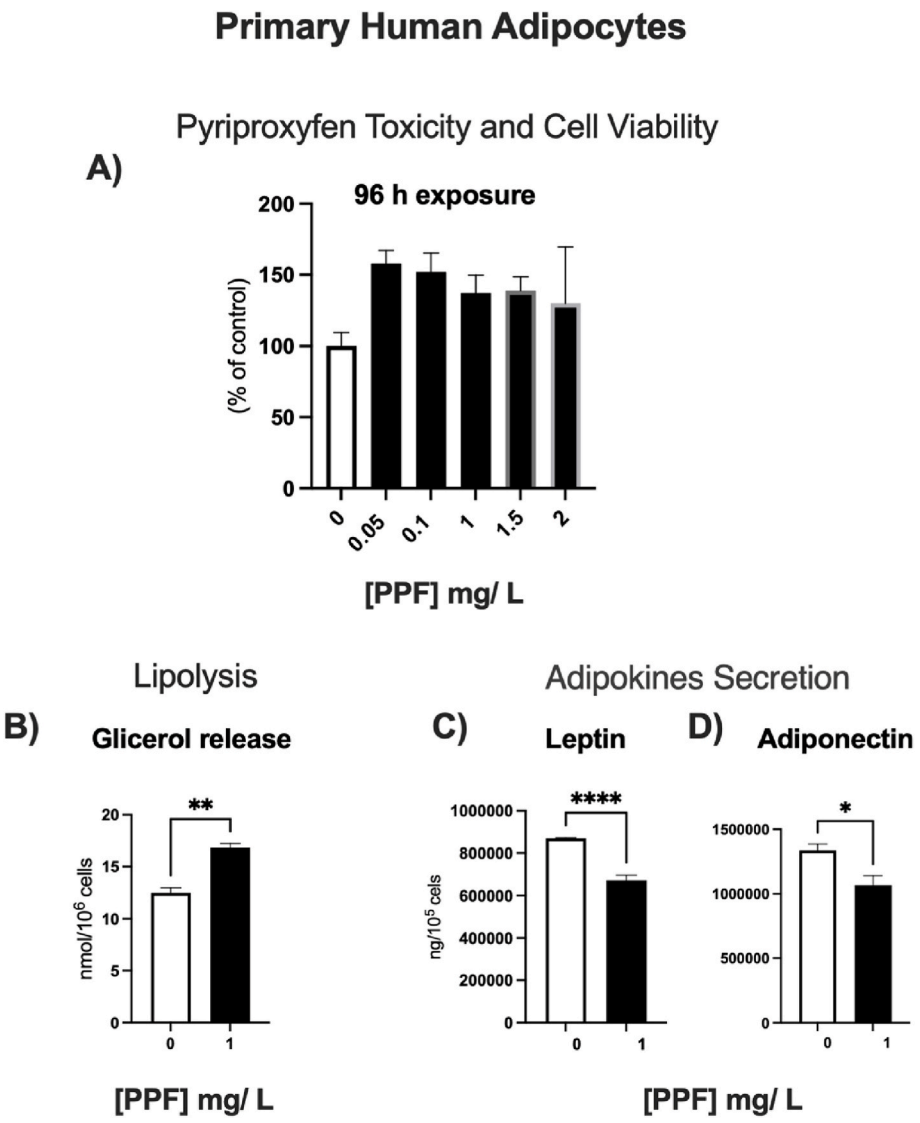

Fig. 5. Cell viability, metabolism and adipokine secretion in human primary adipocytes exposed to PPF. **(A)** Cytotoxicity of PPF in human primary adipocytes isolated from vWAT. Cell viability was assessed by MTT assay after exposure to increasing concentrations (0.05–2 mg/L) of PPF for 96 h. Data are expressed as a percentage of the control (untreated) group. **(B)** Basal lipolysis measured as glycerol release in primary adipocytes after exposure to PPF (1 mg/L). **(C-D)** Secreted levels of leptin and adiponectin from primary adipocytes exposed to PPF (1 mg/L). Mean ± SEM from n = 4 independent human donors (biological replicates), each assayed in technical triplicate. $*p < 0.05$, $**p < 0.001$, $****p < 0.00001$ (One-way ANOVA followed by Tukey's post-test).

classifying it as an indirect mutagen (Bugda et al., 2023). In zebrafish, PPF acts as a neurotoxicant by inhibiting acetylcholinesterase and, critically, by impairing mitochondrial function—leading to energy depletion, calcium dysregulation, and a surge in mitochondrial ROS (Azevedo et al., 2021). This direct link to mitochondrial-derived ROS offers a plausible source for the oxidative stress we observed in hASCs.

Similarly, studies on DFB delineate a cascade initiated by ROS. In bovine mammary epithelial cells, DFB exposure triggers a sustained oxidative burst that activates pro-inflammatory and pro-apoptotic JNK signalling while suppressing pro-survival PI3K/AKT pathways, culminating in mitochondrial failure and cell death (Lee et al., 2021). This pattern of redox-driven signalling reprogramming is consistent with our findings of inflammatory activation (via KDM6B/CCL2) and points to an altered state of cellular homeostasis.

Furthermore, the relevance of combined exposures and developmental toxicity is highlighted by a study in zebrafish embryos, where both PPF and DFB—individually and in mixtures—induced mortality, teratogenicity, and a consistent increase in embryonic ROS levels (Teixeira et al., 2024). This underscores oxidative stress as a conserved mechanism of toxicity across life stages and models, reinforcing the pathophysiological relevance of the redox imbalance we report in human progenitor cells. Together, this literature substantiates the capacity of both pesticides to disrupt fundamental cellular processes, with oxidative stress as a central mediator. Our study extends this paradigm to human adipose biology by demonstrating that non-cytotoxic concentration alters the epigenetic and transcriptional landscape of hASCs, steering them toward a proinflammatory and dysfunctional adipogenic fate. This novel endpoint bridges the gap between cellular oxidative damage and the risk of metabolic tissue dysfunction.

In conclusion, this study provides the first evidence that exposure to non-cytotoxic concentrations of the widely used pesticides PPF and DFB disrupts fundamental processes in hASCs directly linking environmental exposure to pathways of adipose tissue dysfunction. Collectively, our findings outline a potential adverse outcome pathway in which pesticide-induced disturbances in redox regulation may activate interconnected epigenetic, inflammatory, and adipogenic signals, appearing to steer hASCs toward a metabolically dysfunctional state. This triad of events (suggested redox imbalance, epigenetic alterations, and

adipogenic disruption) offers a preliminary mechanistic framework for understanding how environmental chemicals may contribute to metabolic disorders.

While these findings offer initial insights in a relevant human primary cell model, we acknowledge that the use of cells from a small sample population of male donors represents a demographically narrow sample, which limits the generalizability of our conclusions. Future studies should expand on these findings using larger and more diverse donor cohorts to specifically assess the impact of variables such as age, sex, and metabolic status on pesticide susceptibility. Given the global use of these pesticides in vector control, our results underscore the need for further investigation into their potential endocrine and metabolic effects in human health to inform more comprehensive environmental and public health risk assessments.

CRediT authorship contribution statement

Ana Beatriz Marques Abel: Writing – original draft, Visualization, Methodology, Investigation, Formal analysis, Data curation, Conceptualization. **Andressa França Sousa Bispo:** Writing – review & editing, Methodology, Investigation, Formal analysis, Conceptualization. **Jussara de Jesus Simao:** Writing – review & editing. **Artur Francisco da Silva Neto:** Writing – original draft, Methodology, Investigation, Conceptualization. **Julia Fernandes Barcella:** Writing – review & editing, Visualization, Methodology, Investigation, Formal analysis, Data curation, Conceptualization. **Lila Missae Oyama:** Writing – review & editing, Methodology, Investigation, Conceptualization. **Bruno Fiorelini Pereira:** Writing – review & editing, Methodology, Investigation, Conceptualization. **Allain Amador Bueno:** Writing – review & editing. **Maria Isabel Cardoso Alonso-Vale:** Writing – review & editing, Writing – original draft, Visualization, Project administration, Funding acquisition, Conceptualization.

Informed consent statement

Informed consent was obtained from all the subjects involved in the study.

Institutional review board statement

This study was approved by the Research Ethics Committee of the Federal University of São Paulo (CEP/UNIFESP Project No. 0268/2022; approval date: June 7, 2022; CAAE: 57087422.8.0000.5505) and conducted in accordance with the ethical principles of the Declaration of Helsinki and the Brazilian National Health Council Resolution No. 466/2012. Authorization for human tissue collection at Hospital São Luiz was granted under Ethics Opinion No. 7.640.160. Written informed consent was obtained from all participants prior to their inclusion in the study.

Funding

This research was funded by the São Paulo Research Foundation (Fundação de Amparo à Pesquisa do Estado de São Paulo—FAPESP; grant numbers 2019/13618-9 and 2025/03363-4), the Brazilian National Council for Scientific and Technological Development (CNPq; Productivity Research Fellowship, Level 1 E, grant number 307296/2023-7), and the Coordination for the Improvement of Higher Education Personnel—Brazil (CAPES; Finance Code 001; CAPES-PRINT fellowship, grant number 88887.979644/2024-00). LMO is CNPq fellowship recipient.

Declaration of competing interest

The authors declare that they have no known competing financial interests or personal relationships that could have appeared to influence the work reported in this paper.

Data availability

Data will be made available on request.

References

Akhter, N., Kochumon, S., Hasan, A., Wilson, A., Nizam, R., Al Madhoun, A., et al., 2022. IFN-γ and LPS induce synergistic expression of CCL2 in monocytic cells via H3K27 acetylation. J. Inflamm. Res. 15, 4291–4302. https://doi.org/10.2147/JIR.S368352.

Azevedo, R.D.S., Falcão, K.V.G., Assis, C.R.D., et al., 2021. Effects of pyriproxyfen on zebrafish brain mitochondria and acetylcholinesterase. Chemosphere 263, 128029. https://doi.org/10.1016/j.chemosphere.2020.128029.

Bellei, B., Migliano, E., Tedesco, M., Caputo, S., Picardo, M., 2017. Maximizing non-enzymatic methods for harvesting adipose-derived stem cells from lipoaspirate: technical considerations and clinical implications for regenerative surgery. Sci. Rep. 7, 10015. https://doi.org/10.1038/s41598-017-10710-6.

Bispo, A.F.S., Simão, J.J., Moraes, M.A., Abel, A.B.M., Plata, V.T.G., Telles, M.M., Santana, A.V., Volpe, P., Armelin-Correa, L.M., Alonso-Vale, M.I.C., 2025. Effects of obesity-associated plasma markers on adipose stem cell function and epigenetic regulation. Obesity 33 (8), 1529–1542. https://doi.org/10.1002/oby.24321.

Bu, C., Xie, Y., Weng, J., Sun, Y., Wu, H., Chen, Y., Ye, Y., Zhou, E., Yang, Z., Wang, J., 2025. Inhibition of JMJD3 attenuates acute liver injury by suppressing inflammation and oxidative stress in LPS/D-Gal-induced mice. Chem. Biol. Interact. 418, 111576. https://doi.org/10.1016/j.cbi.2025.111576.

Bugda, H., Guven Ezer, B., Rencuzogullari, E., 2023. In vitro screening of genotoxicity and mutagenicity of pyriproxyfen in human lymphocytes and Salmonella typhimurium TA98 and TA100 strains. Drug Chem. Toxicol. 46 (5), 955–961. https://doi.org/10.1080/01480545.2022.2113096.

Cabral, A.P., Maia, F.P.D.S., Magliano, D.C., et al., 2024. Pyriproxyfen, villain or good guy? A brief review. Arch. Endocrinol. Metab. 68 (Spec Issue), e240154. https://doi.org/10.20945/2359-4292-2024-0154.

Chen, X., Xiu, M., Xing, J., Yu, S., Min, D., Guo, F., 2017. Lanthanum chloride inhibits LPS-mediated expression of pro-inflammatory cytokines and adhesion molecules in HUVECs: involvement of NF-κB–JMJD3 signaling. Cell. Physiol. Biochem. 42 (5), 1713–1724. https://doi.org/10.1159/000479439.

de Abreu, G.B.A., Gouveia, A.S., Ferreira, F.A.D.S., et al., 2025. Mosquito-disseminated diflubenzuron and spinosad as alternatives to mosquito-disseminated pyriproxyfen: a proof-of-concept, blind, controlled comparison in experimental cages. Mem. Inst. Oswaldo Cruz 120, e250160. https://doi.org/10.1590/0074-02760250160.

Denizot, F., Lang, R., 1986. Rapid colorimetric assay for cell growth and survival. J. Immunol. Methods 89 (2), 271–277. https://doi.org/10.1016/0022-1759(86)90368-6.

Engin, A., 2024. Adiponectin resistance in obesity: adiponectin leptin/insulin interaction. Adv. Exp. Med. Biol. 1460, 431–462. https://doi.org/10.1007/978-3-031-63657-8_15.

Fei, W., Shui, G., Zhang, Y., et al., 2011. A role for phosphatidic acid in the formation of "supersized" lipid droplets. PLoS Genet. 7 (7). https://doi.org/10.1371/journal.pgen.1002201.

Gao, D., Bing, C., Griffiths, H.R., 2025. Disrupted adipokine secretion and inflammatory responses in human adipocyte hypertrophy. Adipocyte 14 (1), 2485927. https://doi.org/10.1080/21623945.2025.2485927.

Han, X., Xu, X., Yu, T., Li, M., Liu, Y., Lai, J., et al., 2022. Diflubenzuron induces cardiotoxicity in zebrafish embryos. Int. J. Mol. Sci. 23 (19), 11932. https://doi.org/10.3390/ijms231911932.

He, C., Larson-Casey, J.L., Gu, L., Ryan, A.J., Murthy, S., Carter, A.B., 2016. Cu,Zn-superoxide dismutase–mediated redox regulation of Jumonji domain-containing 3 modulates macrophage polarization and pulmonary fibrosis. Am. J. Respir. Cell Mol. Biol. 55 (1), 58–71. https://doi.org/10.1165/rcmb.2015-0183OC.

Jackson, E., Shoemaker, R., Larian, N., Cassis, L., 2017. Adipose tissue as a site of toxin accumulation. Compr. Physiol. 7 (4), 1085–1135. https://doi.org/10.1002/cphy.c160038.

Kietzmann, T., Petry, A., Shvetsova, A., Gerhold, J.M., Görlach, A., 2017. The epigenetic landscape related to reactive oxygen species formation in the cardiovascular system. Br. J. Pharmacol. 174 (12), 1533–1554. https://doi.org/10.1111/bph.13792.

Lecoutre, S., Rebière, C., Maqdasy, S., et al., 2025. Enhancing adipose tissue plasticity: progenitor cell roles in metabolic health. Nat. Rev. Endocrinol. 21 (5), 272–288. https://doi.org/10.1038/s41574-024-01071-y.

Lee, W., An, G., Park, H., Lim, W., Song, G., 2021. Diflubenzuron leads to apoptotic cell death through ROS generation and mitochondrial dysfunction in bovine mammary epithelial cells. Pestic. Biochem. Physiol. 177, 104893. https://doi.org/10.1016/j.pestbp.2021.104893.

Lin, S., Zhong, L., Chen, J., Zhao, Z., Wang, R., Zhu, Y., et al., 2023. GDF11 inhibits adipogenesis of human adipose-derived stromal cells through the ALK5/KLF15/β-catenin/PPARγ cascade. Heliyon 9 (2), e13088. https://doi.org/10.1016/j.heliyon.2023.e13088.

Matar, D.B., Zhra, M., Nassar, W.K., Altemyatt, H., Naureen, A., Abotouk, N., Elahi, M.A., Aljada, A., 2025. Adipose tissue dysfunction disrupts metabolic homeostasis: mechanisms linking fat dysregulation to disease. Front. Endocrinol. 16, 1592683. https://doi.org/10.3389/fendo.2025.1592683.

Morigny, P., Houssier, M., Mouisel, E., Langin, D., 2016. Adipocyte lipolysis and insulin resistance. Biochimie 125, 259–266. https://doi.org/10.1016/j.biochi.2015.10.024.

Nimet, J., Leite, N.F., Paulin, A.F., et al., 2021. Detection of pyriproxyfen bioaccumulation in adipose tissue. Bull. Environ. Contam. Toxicol. 107 (5), 911–916. https://doi.org/10.1007/s00128-021-03356-8.

Obradovic, M., et al., 2021. Leptin and obesity: role and clinical implication. Front. Endocrinol. 12, 585887. https://doi.org/10.3389/fendo.2021.585887.
Porretta, D., Fotakis, E.A., Mastrantonio, V., et al., 2019. Focal distribution of diflubenzuron resistance mutations in Culex pipiens. Acta Trop. 193, 106–112. https://doi.org/10.1016/j.actatropica.2019.02.024.
Qin, S., Hu, J., 2023. Fate and dietary risk assessment of pyriproxyfen. Environ. Sci. Pollut. Res. Int. 30 (3), 7030–7039. https://doi.org/10.1007/s11356-022-22129-2.
Rodbell, M., 1964. Metabolism of isolated fat cells. J. Biol. Chem. 239 (2), 375–380. https://doi.org/10.1016/S0021-9258(18)51687-2.
Schreiner, M., Moreira, R.G., Hulan, H.W., 2006. Positional distribution of fatty acids in egg yolk lipids. J. Food Lipids 13, 36–56. https://doi.org/10.1111/j.1745-4522.2006.00033.x.
Simão, J.J., de Sousa Bispo, A.F., Plata, V.T.G., Abel, A.B.M., Telles, M.M., Armelin-Correa, L.M., Alonso-Vale, M.I.C., 2024. Fish oil attenuates the expression of the CCL2 chemokine and histone-modifying enzymes in LPS-stimulated human preadipocytes. Metabol. Open 24, 100336. https://doi.org/10.1016/j.metop.2024.100336.
Suchanecka, M., Grzelak, J., Farzaneh, M., et al., 2025a. Adipose derived stem cells: sources and differentiation capacity. Biomed. Pharmacother. 186, 118036. https://doi.org/10.1016/j.biopha.2025.118036.
Suchanecka, M., Grzelak, J., Farzaneh, M., et al., 2025b. Adipose derived stem cells: sources and differentiation capacity. Biomed. Pharmacother. 186, 118036. https://doi.org/10.1016/j.biopha.2025.118036.
Sun, J., Sun, X., Chen, J., et al., 2021. microRNA-27b prevents sepsis via JMJD3/NF-κB signaling. Stem Cell Res. Ther. 12 (1), 14. https://doi.org/10.1186/s13287-020-02068-w.
Teixeira, J.R.S., de Souza, A.M., Macedo-Sampaio, J.V., et al., 2024. Embryotoxic effects of pesticides in zebrafish. Toxics 12 (2), 160. https://doi.org/10.3390/toxics12020160.
Ur Rahman, A., Khan, I., Usman, A., Khan, H., 2024. Evaluation of insect growth regulators as biological pesticides. J. Vector Borne Dis. 61 (1), 129–135. https://doi.org/10.4103/0972-9062.392257.
World Health Organization, 2022a. Chemical Fact Sheets: Pyriproxyfen. WHO, Geneva. Available at: https://www.who.int/publications/m/item/chemical-fact-sheets–pyriproxyfen. (Accessed 3 March 2026).
World Health Organization, 2022b. Guidelines for drinking-water Quality: Fourth Edition Incorporating the First and Second Addenda. WHO, Geneva. Available at: https://www.who.int/publications/i/item/9789240045064. (Accessed 3 March 2026).
World Health Organization, 2023. WHO Tool for Benchmarking Ethics Oversight of health-related Research Involving Human Participants. WHO, Geneva. Available at: https://www.who.int/publications/i/item/9789240076426. (Accessed 3 March 2026).
Zorov, D.B., Juhaszova, M., Sollott, S.J., 2014. Mitochondrial reactive oxygen species (ROS) and ROS-induced ROS release. Physiol. Rev. 94 (3), 909–950. https://doi.org/10.1152/physrev.00026.2013.